STABLE TEARING IN AIRCRAFT MATERIAL

Mohd Fairuz Ab Rahman*, Reza D. Mohammed*, Xiaobo Yu, Qianchu Liu**, Graham Clark***

***School of Aerospace, Mechanical and Manufacturing Engineering, RMIT University, Bundoora, Victoria 3083, Australia**

****Defence Science and Technology Organisation, 506 Lorimer Street, Fishermans Bend, Victoria 3207, Australia**

Abstract

Fractographic analysis of fatigue fracture surfaces sometimes reveals bands of tearing, macroscopically visible as crescent-shaped growth zones interposed between fatigue crack growth regions. This paper shows that these bands may appear as a result of constant-amplitude and variable-amplitude load excursions. Essentially, tearing causes the crack-front to advance substantially, in a single load cycle. It also evaluates the significance of K in influencing the depth of tearing, on aerospace aluminium alloy fracture surfaces, produced under constant-amplitude and variable-amplitude fatigue loading. The results show that, at equivalent K, the constant-amplitude loading produces smaller tearing depth than in variable-amplitude loading.

1 Introduction

Fractographic analysis of fatigue fracture surfaces is used extensively [1] in aircraft accident investigation to correlate diverse progression markings which reveal the crack front position, with the load cycle history which was experienced by the failed component in service. However, bands of stable tearing are often observed [2-5] on fracture surfaces of aircraft components, and if these bands are large, their presence can complicate the fractographic analysis.

Stable tearing is visible macroscopically as bands of crescent-shaped crack growth [6] that interrupt fatigue crack growth regions, and has been claimed [4,7] to initiate when the maximum stress intensity factor, K_{max} exceeds the plane strain fracture toughness, K_{Ic}. This transitory instability condition can be achieved during occasional high load cycles [2], or during constant-amplitude loadings [8].

Substantial crack-front advancement as a result of tearing is not yet incorporated in fatigue predictive models, so the influence of tearing on fatigue crack growth is not yet predictable. This paper describes experimental programs which provide some insight into the influence of stress intensity factor, K on the constant-amplitude (CA) and variable-amplitude (VA) tearing depth (Δa) in an aerospace aluminium alloy.

2 Experimental Details

2.1 Material

The 7075-T651 aluminium alloy was used in this study; typical chemical compositions and static mechanical properties of this alloy are shown in Table 1.

Table 1. Typical chemical composition and static mechanical properties (in the rolling direction) of 7075-T651 aluminium alloy at room temperature [9].

	Zn	Cu	Cr	Mg
Principal alloying element, % by weight	5.6	1.6	0.23	2.5

Yield strength, σ_{YS} (MPa)	Ultimate strength, σ_{UT} (MPa)	Elongation, ε_f (%)	Fracture toughness, K_{Ic} (MPa$\sqrt{m}$)
505	570	11	29

2.2 Specimen

The compact tension (CT) configuration was adopted and specimens designed according to ASTM E 399 [10]. The specimens had an average thickness, B and width, W of 6.50 ± 0.01 mm and 40.00 ± 0.05 mm respectively. The crack plane orientation for all specimens was longitudinal-transverse (L-T).

2.3 Experimental Procedure

All tests were conducted on a 100 kN capacity servo-hydraulic fatigue machine, set at load range 20 kN. Details of cyclic loads are shown in Table 2. Specimens A – F were exposed to CA (constant P_{min} and P_{max}) cyclic loads, while specimens G – K were programmed with VA load excursions (CA background with intermittent tensile overloads, P_{ol}).

Table 2. Cyclic loading spectra. CA and VA cyclic loads for specimens A – F and G – K respectively.

Specimen	A	B	C	D	E	F
P_{min} (kN)	0.2	0.3	0.4	0.5	1.2	0.4
P_{max} (kN)	2.0	3.0	4.0	5.0	4.0	4.0
Cycles/second	5	10	10	10	10	5

Specimen	G	H	I	J	K
P_{min} (kN)	0.2	0.2	0.2	0.2	0.2
P_{max} (kN)	2.0	2.0	2.0	2.0	2.0
P_{ol} (kN)	3.0	3.5	4.0	4.0	5.0
Cycles/second	5	5	5	5	5

All specimens in VA loading programs failed by overload, except specimen J and K which failed during the CA background cyclic loading.

2.4 Fracture Surface Examination and Measurement

Tearing was examined using a digital microscope with a magnification between 20 and 400 times. Fig. 1(a) shows an example of a fatigue fracture surface. The area of tearing on the fracture surface was sketched in computer aided design (CAD) program (Fig. 1(b)), to allow recording of crack depth, a (from notch tip) and estimation of crack-front length, l (Fig. 1(c)).

3 Results

3.1 Determination of stress intensity factor, K

As shown in Fig. 1(c), the measured crack depth, a, represented the maximum crack length, even in cases where a substantially curved crack front occurred. The K was determined according to ASTM E 399 [10] from the maximum crack depth and load information (P_{max} in CA and P_{ol} in VA), and results are shown in Table 3. This procedure naturally leads to a notional value for K in cases where there was substantial curvature of the crack front before or after tearing.

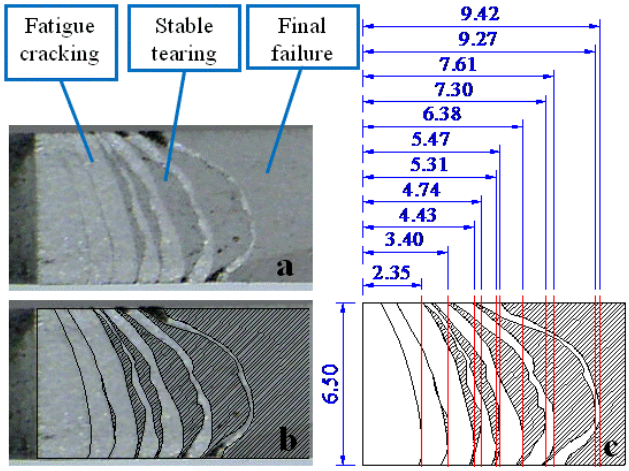

Fig. 1. Examination and measurement of tearing on fracture surface (specimen H); (a) macrograph of fracture surface captured by digital microscope, (b) sketch of tearing in CAD program and (c) measuring the crack depth, a. Crack growth is from left to right.

3.2 Classification and Notation of Tearing

Multiple macroscopic tear bands on the fracture surface of each specimen were numbered according to the sequence of occurrence, such that the first tearing on specimen H (Fig. 1) was marked as H-1. The final tear, which led to final failure, was indicated with capital F next to the specimen code, as shown in Table 3.

The parameters (a, l and K) at onset and arrest of tearing are denoted with subscript i and j respectively. For each tear, the tearing depth, Δa is defined as $a_j - a_i$.

Table 3. Details of measured parameters of tearing.

Tear No.	a (mm)		l (mm)		K (MPa√m)	
	a_i	a_j	l_i	l_j	K_i	K_j
A-1	28.5	29.1	7.3	7.8	35.4	38.5
A-2	29.3	30.2	7.7	8.6	39.9	45.5
A-F	30.9		8.6		51.5	
B-1	25.4	25.6	1.2	1.3	36.5	37.2
B-2	25.8	26.1	6.8	7.1	38.1	39.3
B-3	26.4	26.6	7.3	7.6	40.5	41.7
B-4	26.9	27.6	7.5	8.4	43.1	47.0
B-5	28.1	29.2	8.5	9.2	50.7	58.5
B-F	29.4		9.2		60.6	
C-1	22.3	23.1	7.0	7.9	35.9	38.4
C-2	23.7	24.3	8.3	9.2	40.6	43.3
C-F	24.6		8.9		44.5	
D-1	19.7	20.4	6.9	7.5	36.4	38.2
D-2	20.8	21.4	7.0	7.7	39.5	41.4
D-3	21.9	22.8	8.7	9.6	43.3	46.9
D-F	23.5		9.4		50.1	
E-1	21.9	22.7	7.5	8.2	34.7	37.1
E-2	22.9	23.3	8.1	8.6	37.9	39.3
E-3	24.0	25.9	8.1	9.8	41.9	51.5
E-F	26.0		9.2		52.0	
F-1	22.3	22.6	7.6	8.1	35.9	37.0
F-2	22.9	23.3	7.9	8.2	37.9	39.2
F-3	23.6	24.3	8.2	9.0	40.6	43.1
F-4	24.4	25.7	8.8	10.0	43.9	50.1
F-F	26.2		10.0		53.3	
G-1	20.4	20.4	6.8	6.8	22.9	22.9
G-2	21.2	21.2	6.8	6.8	24.4	24.4
G-3	22.1	22.1	6.8	6.8	26.5	26.5
G-4	22.3	22.3	6.7	6.7	27.0	27.0
G-5	23.1	23.3	6.7	6.9	29.0	29.4
G-6	24.7	26.0	6.8	8.0	33.9	38.8
G-7	27.1	30.0	6.9	10.0	44.0	66.9
G-F	30.1		9.1		68.0	
H-1	20.4	20.4	6.8	6.8	26.7	26.7
H-2	21.4	21.4	7.0	7.0	29.1	29.1
H-3	22.4	22.7	7.0	7.3	31.8	32.7
H-4	23.3	23.5	7.2	7.5	34.4	34.9
H-5	24.4	25.3	7.5	8.5	38.2	42.0
H-6	25.6	27.3	8.0	10.1	43.5	52.8
H-F	27.4		9.0		53.8	
I-1	20.3	20.6	6.8	7.0	30.3	31.2
I-2	21.4	23.2	6.6	8.4	33.1	38.8
I-3	23.3	25.3	7.2	9.7	39.2	47.8
I-F	25.8		9.6		50.8	
J-1	18.9	19.0	4.7	4.8	27.4	27.5
J-2	20.0	20.2	6.6	6.7	29.7	30.1
J-3	20.6	20.8	7.3	7.4	31.1	31.6
J-4	21.6	22.9	6.8	8.0	33.8	38.0
J-5	23.3	24.8	7.6	9.0	39.4	45.5
J-6	28.9	29.5	7.7	8.3	37.6	41.1
J-7	29.6	30.0	8.2	8.5	41.6	44.5
J-F	30.2		8.4		46.1	
K-1	20.4	22.8	6.9	10.0	38.2	46.7
K-2	28.5	29.2	7.1	7.8	35.5	39.0
K-3	29.9	30.8	7.6	8.7	43.4	50.3
K-F	31.2		8.7		54.7	

4 Discussions

4.1 Crack front curvature

The tearing can lead to a substantially curved crack front, and an increase in the crack-front length. This change is associated with a return to "normal" fatigue crack growth, and Vlasveld and Schijve [4] proposed correction factors for K after tearing, based on fracture mechanics concepts, in which the trailing ligaments of uncracked material retard crack advance, progressively, as the front tunnels ahead, until the increased resistance to advance prevents further tearing and causes the return to fatigue crack growth.

Forsyth [8] used a simpler approximation, proposing that the additional crack front line length could be linked to the stress intensity factor and used to provide a suitable correction for the tunnelling. A similar approach has been adopted by Neale [11] to estimate the K-value for the thumbnail crack under static loading conditions.

As indicated above, extensive tearing leads to a curved crack-front and a temporary reduction in crack growth rate (Bowen and Forsyth [12] found that an increase in 20% of crack-front length could cause a 30% reduction in ΔK) or an increase in the material's ability to sustain higher load [13].

It is emphasised that the evaluation of stress intensity factors in Table 3 utilised the maximum crack depth, a, which often occurred near the mid-thickness of the specimen. As tearing always results in crack tunnelling, K is only a notional value where tunnelling is extensive.

Ab Rahman et al. [14] noted that, the determination of actual K-value for curved crack-front is still not well-established; however, an attempt has been made by Liu et al. [15] to use finite element analysis to model the variation of K along the crack-front curvature. Essentially, the curved crack-front would cause the *real* K at the deepest part of the crack to be lower than this estimated "notional" K based on the maximum crack depth [4,7]. This discrepancy has been suggested [13,16] to be small, although extensive crack front

"tunnelling" would clearly accentuate the effect. At this stage (prior to detailed finite element analysis) the notional values of K have been adopted for the purpose of comparing the CA and VA test conditions.

4.2 Relationship between stress intensity factor, K and tearing depth, Δa

To assess the differences between CA and VA tearing, the effect of K_i on Δa was assessed from the results in Table 3. Fig. 2 shows three things:

- Generally, for similar K, the CA tearing at initiation has smaller Δa than the VA tearing.
- The K at the onset of VA tearing onset is lower than that required under CA loading.
- The size of VA tearing is markedly larger than that sustainable under CA.

These results suggest that the CA loading is conferring some resistance to tearing. This resistance seems logical if we consider that the cycles immediately before the tearing onset are much larger in the CA case, and this may lead to a variety of changes. Cyclic hardening or softening of the material near the crack tip may occur, and the high prior loading can also induce residual stresses or crack tip blunting, and these changes could contribute to increased resistance to tearing.

An alternative view of the apparent tearing resistance, however, is that the K at tearing onset cannot be established as corresponding to the maximum load P_{ol} in the overload cycle; it may be that the tearing onset occurs part-way up the overload cycle, allowing the tearing extent, Δa to be much larger in VA.

5 Conclusions

There is clearly significant complexity in determining the actual K for the curved crack-fronts associated with tearing, and while empirical correction has been proposed by several authors, the next step in the current research will be to undertake detailed analysis of the stress intensity factors applicable to the observed tearing geometries. The VA tearing starts at lower K_i than the CA, and the VA tearing is more likely to produce larger Δa than the CA tearing, at about the same K_i. In effect, the CA conditions provide an apparent resistance to tearing. The discrepancies in Δa between these two loading arrangements are believed to be associated with the high loads in the CA loading immediately prior to tearing. Possible effects of these high loads may induce cyclic hardening or softening of the material near the crack tip, residual stresses or crack tip blunting.

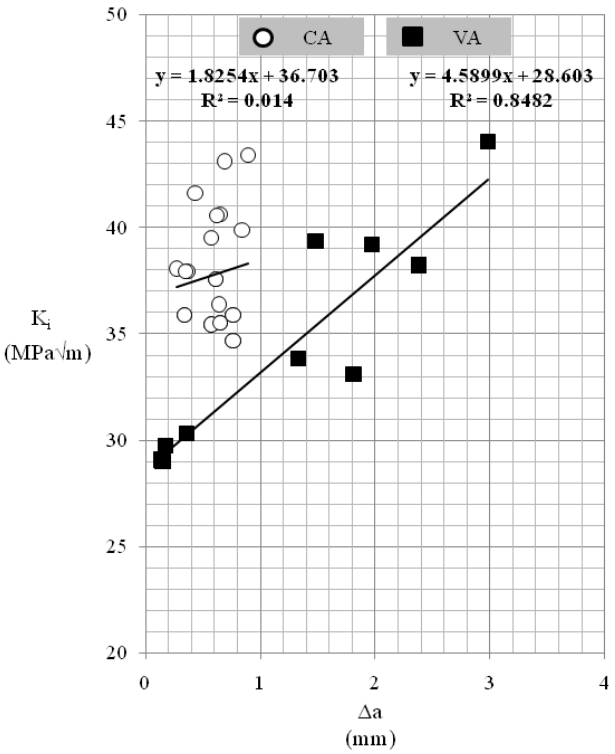

Fig. 2. Effect of K_i the notional stress intensity factor at initiation of tearing, on the extent of tearing Δa.

References

[1] Goldsmith NT and Clark G. Fractographic techniques for the assessment of aircraft component cracking. In: Berkovits A, editor. *Aeronautical fatigue in the electronic era*. Engineering Materials Advisory Services, pp 199-214, 1989.

[2] Hudson CM and Hardrath HF. *Investigation of the effects of variable-amplitude loadings on fatigue crack propagation patterns*. National Aeronautics and Space Administration, Technical Note D-1803, 1963.

[3] McIntyre D. Fractographic analysis of fatigue failures. *Journal of Engineering Materials and Technology*, Vol. 97, pp 194-205, 1975.

[4] Vlasveld JA and Schijve J. Tongue-shaped crack extension during fatigue of high strength aluminium alloys. *Fatigue of Engineering Materials and Structures*, Vol. 3, pp 129-145, 1980.

[5] Goldsmith NT, Clark G and Barter SA. A growth model for catastrophic cracking in an RAAF aircraft. *Engineering Failure Analysis*, Vol. 3, No. 3, pp 191-201, 1996.

[6] Forsyth PJE and Ryder DA. Some results of the examination of aluminium alloy specimen fracture surfaces. *Metallurgia*, Vol. 63, No. 377, pp 117-124, 1961.

[7] Bowen AW and Forsyth PJE. On the mechanism of mixed fatigue-tensile crack growth. *Materials Science and Engineering*, Vol. 49, No. 2, pp 141-154, 1981.

[8] Forsyth PJE. Causes of mixed fatigue-tensile-crack growth and significance of microscopic crack behaviour. *Metals Technology*, Vol. 5, No. 10, pp 351-357, 1978.

[9] Dowling NE. *Mechanical behaviour of materials – Engineering methods for deformation, fracture, and fatigue*. 3rd edition, Pearson Education, 2007.

[10] ASTM E 399 – 06. Standard test method for linear-elastic plane-strain fracture toughness K_{Ic} of metallic materials. In: *Annual Book of ASTM Standards*, Vol. 03.01, ASTM International, pp 498-529, 2008.

[11] Neale BK. An investigation into the effect of thickness on the fracture behaviour of compact tension specimens. *International Journal of Fracture*, Vol. 14, No. 2, pp 203-212, 1978.

[12] Bowen AW and Forsyth PJE. The effect of frequency changes on fatigue crack growth in 7178-T6 aluminium alloy. *Fourth International Conference on Fracture*, Waterloo, Vol. 2, pp 1217-1222, 1977.

[13] Neale BK. The influence of crack shape on fracture toughness testing. *International Journal of Fracture*, Vol. 12, No. 3, pp 499-502, 1976.

[14] Ab Rahman MF, Mohammed RD, Yu X, Liu Q and Clark G. Assessment of stable tearing on fatigue fracture surfaces. *Engineering Failure Analysis*, in press, 2010.

[15] Liu Q, Hamel P, Hu W, Sharp PK, Lahousse A and Clark G. *Modelling of stable tearing in aircraft structures*. Defence Science and Technology Organisation, Technical Report DSTO-TR-1657, Victoria, 2005.

[16] Petrak GJ. A note on fatigue crack front straightness in K_{Ic} testing. *Engineering Fracture Mechanics*, Vol. 4, No. 2, pp 311-313, 1972.

Contact Author Email Address

s3216571@student.rmit.edu.au

Copyright Statement